N91-17092

GAMMA RAY OBSERVATORY (GRO) OBC ATTITUDE ERROR ANALYSIS

by
R. R. Harman
NASA - Goddard Space Flight Center
Greenbelt, MD 20771

ABSTRACT

This analysis involves an in-depth look into the OBC attitude determination algorithm. A review of TRW error analysis and necessary ground simulations to understand the onboard attitude determination process are performed. In addition, a plan is generated for the in-flight calibration and validation of OBC computed attitudes. Pre-mission expected accuracies are summarized and sensitivity of onboard algorithms to sensor anomalies and filter tuning parameters are addressed.

1.0 INTRODUCTION

The Gamma Ray Observatory (GRO) (see Reference 10) is a three axis stabilized spacecraft scheduled to be launched into a 350-450 Km orbit 1990 by the Space Transportation System (STS). The GRO science instruments study gamma ray sources between 0.1 to 30000 mega-electron-volts (MeV) before they are absorbed by the Earth's atmosphere. The spacecraft is designed to stay inertially pointed, using reaction wheel control, for two weeks at a time before maneuvering to the next gamma ray target.

GRO has an onboard attitude determination accuracy requirement of 86.4 arcseconds per axis (3 sigma) during the normal science observation mode. This accuracy is accomplished by the use of two Fixed Head Star Trackers (FHSTs) and an Inertial Reference Unit (IRU). Both of these attitude sensors have been used on the Solar Maximum Mission (SMM), LANDSAT 4, and LANDSAT 5 spacecraft. As a backup, the Fine Sun Sensor (FSS) can take the place of a FHST with the resultant attitude accuracy of 167.5 arcseconds/axis (3 sigma). In both cases, the attitude is propagated using the IRU data and updated after a FHST or FSS measurement by using an extended Kalman Filter.

2.0 GRO ONBOARD ATTITUDE ESTIMATION (Reference 1)

Time Propagation

In GRO, the attitude computations are contained in two modules: kinematic integration module and attitude estimation module. The kinematic integration routine uses the previous cycle OBC quaternion and the current gyro output to update the OBC quaternion. The kinematic equation for updating a quaternion is (Reference 2):

$$q(t_{n+1}) = \left\{ \cos(wT/2)\ I + 1/w \sin(wT/2) \begin{vmatrix} 0 & w_z & -w_y & w_x \\ -w_z & 0 & w_x & w_y \\ w_y & -w_x & 0 & w_z \\ -w_x & -w_y & -w_z & 0 \end{vmatrix} \right\} q(t_n) \quad \ldots 2.1$$

where $w = (w_x^2 + w_y^2 + w_z^2)^{1/2}$
T = time interval
I = 4x4 identity matrix.

Since the gyro output consists of three angles θ_x, θ_y, θ_z the following substitutions can be made:

$$\theta_x = w_x T, \ \theta_y = w_y T, \ \theta_z = w_z T$$

Equation 2.1 then becomes:

$$q(t_{n+1}) = \left\{ \cos(\theta/2) \ I + 1/\theta \sin(\theta/2) \begin{vmatrix} 0 & \theta_z & -\theta_y & \theta_x \\ -\theta_z & 0 & \theta_x & \theta_y \\ \theta_y & -\theta_x & 0 & \theta_z \\ -\theta_x & -\theta_y & -\theta_z & 0 \end{vmatrix} \right\} q(t_n) \quad \ldots 2.2$$

where $\theta = (\theta_x^2 + \theta_y^2 + \theta_z^2)^{1/2}$

Every 32.768 seconds, the attitude estimation routine (ATTEST) generates roll, pitch, and yaw errors. These errors are fed into the kinematic integration routine in place of the normal gyro data that is used between 32.768 second updates.

The attitude estimation routine (ATTEST) itself consist of an extended Kalman filter (KF). Reference 1 contains an outline of ATTEST. The KF is implemented in two steps. First, the propagation of the internal statistics based on the Dynamics Model and second, updating the state vector based on the Observation Model, the measurements, and the internal statistics. ATTEST alternates between the two sensors (FHST/FHST or FHST/FSS) being used for attitude estimation every 32.768 seconds.

Dynamics Model

The gyro rate measurement is assumed to have the following form:

$$\dot{\underline{\theta}} = \underline{w} + \underline{b}_o + \underline{b} - \underline{n}_v$$

$$\dot{\underline{b}} = \underline{n}_u$$

where, $\dot{\underline{\theta}}$ - gyro rate measurement
$\underline{w}$ - true spacecraft rate
$\underline{b}_o$ - gyro bias error
$\underline{b}$ - gyro random walk error
$\underline{n}_v$ - float torque noise (gaussian white noise)
$\underline{n}_u$ - float torque derivative noise (gaussian white noise)

The gyro drift error, $\dot{e}$, is defined as follows:

$$\dot{\underline{e}} = \underline{w} - \dot{\underline{\theta}}$$

It then becomes the following equation:

$$\dot{\underline{e}} = -\underline{b}_o - \underline{b} + \underline{n}_v$$

The gyro bias $\underline{b}_o$ is assumed to be known and can be taken out of the above equation. Therefore:

$$\dot{\underline{e}} = -\underline{b} + \underline{n}_v$$

$$\dot{\underline{b}} = \underline{n}_u$$

The attitude error, $\underline{\Psi}$, is computed as follows:

$$\dot{\underline{\Psi}} + \underline{w} \times \underline{\Psi} = \dot{\underline{e}}$$

However since $\underline{w}$ is neglible, the dynamic model is reduced to the following form:

$$\dot{\underline{\Psi}} = -\underline{b} + \underline{n}_v$$

$$\dot{\underline{b}} = \underline{n}_u$$

If these two equations are put into a linear state space formulation equations (2.3) and (2.4) are derived:

$$\dot{\underline{X}}(t) = F\,\underline{X}(t) + \underline{W}(t) \tag{2.3}$$

$$\dot{\underline{X}}(t) = \begin{vmatrix} \dot{\underline{\Psi}} \\ \dot{\underline{b}} \end{vmatrix} = \begin{vmatrix} \underline{0}_{3x3} & -\underline{I}_{3x3} \\ \underline{0}_{3x3} & \underline{0}_{3x3} \end{vmatrix} \begin{vmatrix} \underline{\Psi} \\ \underline{b} \end{vmatrix} + \begin{vmatrix} \underline{n}_{v(3x1)} \\ \underline{n}_{u(3x1)} \end{vmatrix} \tag{2.4}$$

where, $\underline{\Psi}$ - attitude error
$\underline{b}$ - gyro random walk error
$\underline{n}_v$ - float torque noise (Gaussian)
$\underline{n}_u$ - float torque derivative noise (Gaussian)

The state equation is discretized to the following form:

$$\underline{X}(t_k) = \Phi_k\,\underline{X}(t_{k-1}) + \underline{W}(t_k)$$

where $\Phi_k = e^{AT_k}$ and $T_k = t_k - t_{k-1}$.

The two characteristics of $\underline{W}(t)$ are the mean:

$$E[\,\underline{W}(t)\,] = 0$$

And the covariance:

$$E[\,\underline{W}(t)\,\underline{W}^T(t')\,] = \begin{vmatrix} \underline{n}_v\underline{n}_v^T & \underline{0}_{3x3} \\ \underline{0}_{3x3} & \underline{n}_u\underline{n}_u^T \end{vmatrix} \delta(t-t') \tag{2.5}$$

where "T" denotes the transpose. Note that the off diagonal elements in (2.5) are zero since it is assumed that there is no correlation between $\underline{n}_u$ and $\underline{n}_v$.

The Spectral Density Matrix is defined as follows:

$$Q(t) = E[\,\underline{W}(t)\,\underline{W}^T(t)\,] \tag{2.6}$$

Thus the covariance is given as

$$Q(t) \int (t-t') \tag{2.7}$$

The discrete Dynamics Noise Covariance matrix, Q_k, is obtained using the state transition matrix, ϕ_k, and the Spectral Density matrix, $Q(t)$, in the following manner:

$$Q_k = \int_{t_{k-1}}^{t_k} \phi(t_k,t') \; Q(t') \; \phi^T(t_k,t') \; dt' \tag{2.8}$$

Once Q_k is computed, it is used to propagate the state covariance matrix as follows:

$$P_k(-) = \phi_k \; P_{k-1}(+) \; \phi_k^T + Q_k \tag{2.9}$$

where $P_k(-)$ is the Propagated Covariance Matrix at time k and,
$P_{k-1}(+)$ is the updated Covariance Matrix at time k-1.

Observation Model

FHST Model

In the GRO Flight Software, the FHST measurements are used to create an observed star unit vector, OS, in the Sensor Coordinate frame. The identified star position in the star catalog is used to create an expected or computed unit star vector, CS, in the Sensor Coordinate Frame. We then define

$$Z_k(i) = OS_k(i) - CS_k(i) \quad \text{for i=x and y} \tag{2.10}$$

where Z_k is the measurement residual.

From this definition of Z_k , H_k is shown to be

$$H_k = \begin{vmatrix} -(\underline{X} \times \underline{S}_k)^T & 0_{1x3} - \\ -(\underline{Y} \times \underline{S}_k)^T & 0_{1x3} - \end{vmatrix} \tag{2.11}$$

where $\underline{S}_k$ is the observed star vector in the spacecraft body frame,
$\underline{X}$ is the X axis of the FHST in the spacecraft body frame,
and $\underline{Y}$ is the Y axis of the FHST in the spacecraft body frame.

In the observation model

$$\underline{Z}_k = H_k \underline{X} + \underline{V}_k \tag{2.12}$$

where $\underline{Z}_k$ is the observation defined in (2.9), and $\underline{V}_k$ is the sensor noise (Gaussian).

The sensor noise characteristics are the following:

$$E[\ \underline{V}_k\ ] = 0 \tag{2.13}$$

$$R_k = E[\ \underline{V}_k\ \ \underline{V}_1{}^T] = \begin{bmatrix} R_{11} & 0 \\ 0 & R_{22} \end{bmatrix} \tag{2.14}$$

It is further assumed that the initial state vector $\underline{X}_o$ is Gaussian and $\underline{X}_o$, $\underline{W}$,and $\underline{V}_k$ are independant of each other. Since all are assumed zero mean and Gaussian, this is equivalent to assuming they are uncorrelated with each other.

FSS Model (Reference 10)

As with the FHST, the FSS model uses an observed Sun position, $\underline{OS}$, and a computed Sun position, $\underline{CS}$, to compute measurement residuals, $\underline{Z}$, as follows:

$$Z_k(i) = OS_k(i) - CS_k(i) \text{ for } i=x \text{ and } y.$$

The measurement equation is the same used for the FHST (2.12). For the FSS, the H_k is shown to be:

$$H_k = \begin{bmatrix} (\underline{X}_{MP} \times \underline{S}_k)^T & 0_{1x3} \\ (\underline{Y}_{MP} \times \underline{S}_k)^T & 0_{1x3} \end{bmatrix} \tag{2.15}$$

where $\underline{S}_k$ is the computed sun vector. $\underline{X}_{MP}$ and $\underline{Y}_{MP}$ are as follows:

$$\begin{aligned}
X_{MPx} &= (X_{Fx} - Z_{Fx}\ XP\ ) / (\hat{\underline{Z}}_F \cdot \underline{S}_k) \\
X_{MPy} &= (X_{Fy} - Z_{Fy}\ XP\ ) / (\hat{\underline{Z}}_F \cdot \underline{S}_k) \\
X_{MPz} &= (X_{Fz} - Z_{Fz}\ XP\ ) / (\hat{\underline{Z}}_F \cdot \underline{S}_k) \\
Y_{MPx} &= (Y_{Fx} - Z_{Fx}\ YP\ ) / (\hat{\underline{Z}}_F \cdot \underline{S}_k) \\
Y_{MPy} &= (Y_{Fy} - Z_{Fy}\ YP\ ) / (\hat{\underline{Z}}_F \cdot \underline{S}_k) \\
Y_{MPz} &= (Y_{Fz} - Z_{Fz}\ YP\ ) / (\hat{\underline{Z}}_F \cdot \underline{S}_k)
\end{aligned}$$

where $\underline{X}_F$ is the FSS X-coordinate axis in the spacecraft frame,
$\underline{Y}_F$ is the FSS Y-coordinate axis in the spacecraft frame,
$\underline{Z}_F$ is the FSS Z-coordinate axis in the spacecraft frame,
XP and YP are the FSS expected measurements.

The FSS noise characteristics are the same as those for the FHST.

Update Algorithms

The state vector is updated by processing the following equation with the inputs $P_k(-)$ (2.9), H_k (2.11 and 2.15), R_k (2.14), and the observation vector Z_k (2.12):

$$K_k = P_k(-)\ H_k^T\ [\ H_k\ P_k(-)\ H_k^T + R_k]^{-1} \tag{2.16}$$

$$P_k(+) = (\ I - K_k\ H_k)\ P_k(-) \tag{2.17}$$

$$\hat{\underline{X}}_k(+) = \hat{\underline{X}}_k(-) + K_k(\ \underline{Z}_k - H_k\ \hat{\underline{X}}_k(-)\ ) \tag{2.18}$$

where $P_k(+)$ is the updated Covariance Matrix.
K_k is the Kalman Gain Matrix.
$\hat{\underline{X}}_k(+)$ is the updated State Vector.

The GRO Flight Software employees a scaler implementation method which requires the sequence of equations (2.16-2.18) to be executed twice. In the first pass the following substitutions are made for the FHSTs (similarly for the FSS):

$$H_k = H_{k,1} = [\ (\ \underline{X} \times \underline{S}_k\ )^T \quad 0_{1x3}\ ]$$
$$R_k = R_{k,1} = R_{11}$$

The resulting Kalman Gain Matrix $K_{k,1} = K_k$ is used to update the covariance matrix (2.17) where $P_{k,1} = P_k$ and the update (2.18) where $\hat{\underline{X}}_k(-) = 0$. The equations are listed below:

$$K_{k,1} = P_k(-)\ H_{k,1}^T\ /\ [\ H_{k,1}\ P_k(-)\ H_{k,1}^T + R_{k,1}\ ]$$
$$P_{k,1}(+) = [\ I - K_{k,1}\ H_{k,1}]\ P_k(-)$$
$$X_{k,1}(+) = K_{k,1}\ Z_{k,1}$$

where $Z_{k,1}$ is the X component of $\underline{Z}_k$.

In the second pass, there are the following substitutions:

$$H_k = H_{k,2} = [\ (\ \underline{Y} \times \underline{S}_k\ )^T \quad 0_{1X3}\ ]$$
$$R_k = R_{k,2} = R_{22}$$
$$K_k = K_{k,2}$$
$$P_k(-) = P_{k,1}(+)$$
$$\hat{\underline{X}}_k(-) = \hat{\underline{X}}_{k,1}(+)$$

where $\hat{\underline{X}}_{k,1}(+)$ is the state vector update from the first pass.

The final Kalman Gain Matrix $K_k = K_{k,2}$ is used to update the covariance matrix and the state vector. The equations are listed below:

$$K_{k,2} = P_k(-)\ H_k^T\ /\ [\ H_k\ P_k(-)\ H_k^T + R_k]$$
$$P_k(+) = [\ I - K_k\ H_k]\ P_k(-)$$
$$\hat{\underline{X}}_k(+) = \hat{\underline{X}}_k(-) + K_k[\ Z_{k,2} - H_k\ \hat{\underline{X}}_k(-)\ ]$$

where $Z_{k,2}$ is the Y component of $\underline{Z}_k$.

3.0 ADEAS

The Attitude Determination Error Analysis System (ADEAS) was the attitude tool used in this analysis. It models state estimation using either a batch filter or a Kalman filter. The ADEAS Kalman filter is the same two pass filter implementation as described for GRO in Section 2.0. Thus, ADEAS provides a convient method for GRO onboard attitude error analysis.

ADEAS models an attitude system by use of consider and solve-for parameters. The solve-for parameters are those the onboard filter uses in its state vector. For GRO, the solve-for state components are the three attitude errors and the three gyro drift errors. The consider parameters are those that the onboard filter does not take in account such as misalignments and scale factor errors.

4.0 ONBOARD ATTITUDE ACCURACY

4.1 Attitude Accuracy Requirement

Using the above attitude estimation algorithm, the overall attitude determination requirement and the TRW stated capabilities are as follows (Reference 3):

	Requirement (arc-sec) (3-sigma)	Capability (arc-sec) (3-sigma)
Attitude determination accuracy using two FHSTs	86.4	71.2
Attitude determination accuracy using 1 FHST and 1 FSS	167.5	143.8

The FHST/FHST algorithm errors were the largest single contributer to the error budget at 53.3 arcseconds/axis. The FSS alignment error of 97.5 arcseconds/axis was the largest contributer to the FHST/FSS error budget. According to TRW error budgets, the absolute attitude determination requirement is met for both cases with a reserve.

ADEAS simulations were conducted to independantly verify that the Onboard attitude determination requirement could be met. According to TRW analysis, the update filter required 3 hours to converge (Reference 3). The simulation length consisted of the three hour convergence time plus one orbit of data. The primary error parameters used in these simulations are listed below:

Input parameters

Dynamic Noise (Reference 3)
White 4.2459E-2 arcseconds/sec$^{1/2}$ per axis
Random walk 4.4413E-5 arcseconds/sec$^{3/2}$ per axis
Misalignments
FHST # 1 32 arcseconds/axis (Table 1)
FHST # 2 32 arcseconds/axis (Table 1)
FSS 97.5 arcseconds/axis (Table 2)
Gyro 56 arcseconds/axis (Reference 4)
Measurement Noise
FHST #1 32.3 arcseconds (Note 1)
FHST #2 32.3 arcseconds (Note 1)
FSS 82.1 arcseconds (Note 2)
Gyro Scale Factor Error (3000 PPM) (Reference 5)
Initial Attitude Error (1800 arcseconds/axis)
Initial Gyro Drift Error (0.5 arcseconds/second/axis)
Systematic Calibration Errors (FHST #1 and FHST #2)
H and V measurements - 7 arcseconds (Reference 6)
Attitude Stabilization Errors 0.096 degrees (Reference 3)
Simulation Length (273.58 minutes)

For each simulation, the algorithm uncertainties and the jitter due to reaction wheel disturbances were RSS'd with the resultant simulation attitude errors in order to compare the simulation results to the error budget.

4.2 FHST/FHST CASE

This case is the nominal configuration for attitude estimation onboard and the most accurate. After the three hour convergence period, the maximum filter roll, pitch, and yaw attitude errors were 64.11, 64.74, and 60.80 arcseconds respectively. The gyro drift errors for the roll, pitch, and yaw axes were 3.335×10^{-3}, 3.356×10^{-3}, 3.899×10^{-3} arcseconds/second respectively. The onboard attitude accuracies are well within the 86.4 arcsecond/axis requirement. From Figure 4.1, steady state convergence occurs approximately 6200 seconds into the simulation.

4.3 FHST/FSS Case

This case is used only if one FHST fails, and the resultant accuracy degrades considerably. After the three hour convergence period, the maximum roll, pitch, and yaw attitude errors were 126.85, 120.13, and 80.12 arcseconds respectively. The roll, pitch, and yaw gyro drift errors were 4.046×10^{-3}, 3.379×10^{-3}, and 6.376×10^{-3} arcseconds/second respectively. The attitude accuracies are well within the 167.5 arcsecond/axis requirement. From Figure 4.2, the steady state convergence occurs at approximately 8800 seconds.

4.4 1 FHST With Two Guide Stars Case

A simulation of 56000 seconds was made using FHST #2 and two guide stars within one degree of the FHST boresight. The stars were measured alternately every 32 seconds. The attitude estimation errors were smaller for this case than for the FHST/FSS case. From Figure 4.3, the convergence time for this simulation was approximately 48000 seconds which is about eight times that of the FHST/FHST case and six times that of the FHST/FSS case. The longer convergence time is understandable from observability reasons alone. The maximum roll, pitch, and yaw attitude estimation errors over the last 8000 seconds of the simulation were 100.34, 100.03, and 64.38 arcseconds respectively. The roll, pitch, and yaw gyro drift error were 5.378×10^{-3}, 5.375×10^{-3}, and 3.382×10^{-3} arcseconds/second respectively.

5.0 SENSITIVITY ANALYSIS

For the sensitivity analysis, the consider parameters used for the ADEAS simulations were increased by a factor of two. The resulting ADEAS attitude errors are RSS'd with the algorithm implementation error and jitter due to the reaction wheels. The case designations were as follows:

[1]From reference 7, the FHST calibration error is 30 arcseconds (3-sigma), and the noise equivalent angle (NEA) is 24 arcseconds (3-sigma). The NEA is reduced to 12 arcseconds by data averaging onboard. The resultant measurement error is the RSS of 30 and 12 arcseconds.

[2]From reference 8, the calibration error is 79.2 arcseconds (3-sigma), and the noise equivalent angle is 21.6 arcseconds. The resultant measurement error is the RSS of 79.2 and 21.6 arcseconds.

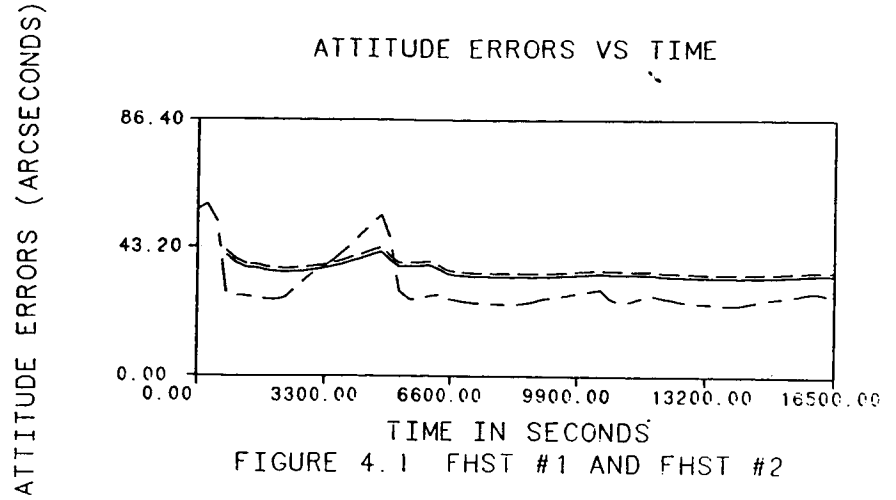

FIGURE 4.1 FHST #1 AND FHST #2

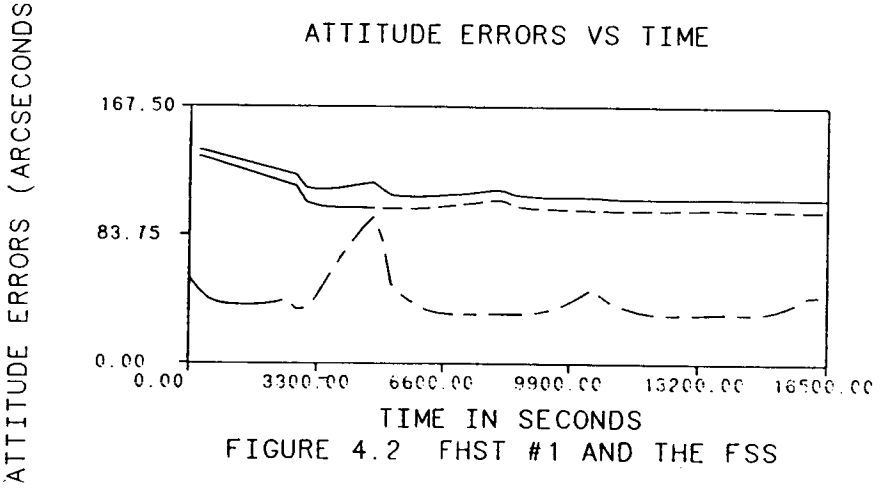

FIGURE 4.2 FHST #1 AND THE FSS

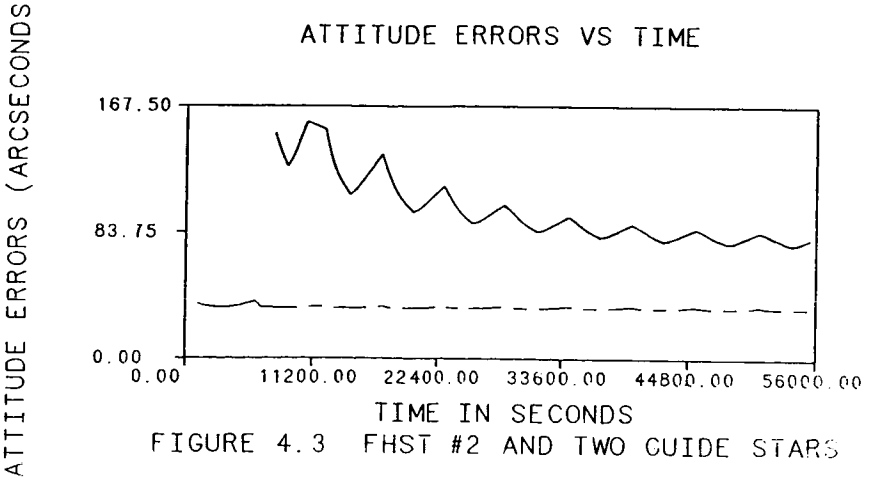

FIGURE 4.3 FHST #2 AND TWO GUIDE STARS

FHST/FHST Configuration

Case	Error Description
1A	Baseline
2A	2x Gyro white noise about each gyro axis
3A	2x Gyro random walk noise about each gyro axis
4A	2x Gyro scale factor error about each gyro axis
5A	2x Gyro misalignment about each gyro axis
6A	2x FHST #1 misalignment about each FHST #1 axis
7A	2x FHST #2 misalignment about each FHST #2 axis
8A	2x FHST noise

FHST/FSS Configuration

Case	Error Description
1B	Baseline
2B	2x Gyro white noise about each gyro axis
3B	2x Gyro random walk noise about each gyro axis
4B	2x Gyro scale factor error about each gyro axis
5B	2x Gyro misalignment about each gyro axis
6B	2x FHST #1 misalignment about each FHST #1 axis
7B	2x FSS misalignment about each FSS axis
8B	2x FHST noise
9B	2x FSS noise
10B	2x FHST and FSS noise

1 FHST with Two Guide Stars Configuration

Case	Error Description
1C	Baseline
2C	2x Gyro white noise about each gyro axis
3C	2x Gyro random walk noise about each gyro axis
4C	2x Gyro scale factor error about each gyro axis
5C	2x Gyro misalignment about each gyro axis
6C	2x FHST #2 misalignment about each FHST axis
7C	2x FHST noise

The attitude error results for the FHST/FHST case are as follows:

Attitude Determination Errors (arcseconds)

Case	Axis	Roll	Pitch	Yaw
1A		64.11	64.74	60.80
2A	x	64.24	64.75	60.80
2A	y	64.23	64.86	60.80
2A	z	64.11	64.74	60.92
3A	x	65.39	64.80	61.22
3A	y	64.18	66.04	61.22
3A	z	64.11	64.74	61.74
4A	x	64.11	64.74	60.80
4A	y	64.11	64.74	60.80
4A	z	64.11	64.74	60.80
5A	x	64.11	64.74	60.80
5A	y	64.11	64.74	60.80
5A	z	64.11	64.74	60.80
6A	x	74.80	76.02	61.22
6A	y	64.00	64.74	74.35
6A	z	64.12	64.74	60.80

7A	x	74.77	76.05	61.22
7A	y	64.12	64.73	75.42
7A	z	64.12	64.74	60.81
8A		65.39	66.10	60.47

The gyro drift error results for the FHST/FHST case are as follows:

Gyro Drift Estimation Errors (10^{-3} arcseconds/second)

Case	Axis	Roll	Pitch	Yaw
1A		3.335	3.356	3.899
2A	x	3.414	3.352	3.899
2A	y	3.332	3.432	3.899
2A	z	3.335	3.356	3.982
3A	x	6.228	3.404	4.414
3A	y	3.385	6.260	4.414
3A	z	3.335	3.356	6.185
4A	x	3.335	3.356	3.899
4A	y	3.335	3.356	3.899
4A	z	3.335	3.356	3.899
5A	x	3.335	3.356	3.899
5A	y	3.335	3.356	3.899
5A	z	3.335	3.356	3.899
6A	x	3.356	3.374	4.414
6A	y	3.165	3.201	6.250
6A	z	3.335	3.356	3.899
7A	x	3.356	3.374	4.414
7A	y	3.356	3.376	5.774
7A	z	3.335	3.356	3.899
8A		3.805	3.859	3.420

The increased gyro white noise and random walk noise about an axis primarily affects that axis as expected. There is some correlation between the X and Y axes but not enough to be significant. Of the two errors, the random walk component proves to affect the attitude errors the most. As expected, the random walk errors contribute the most to the gyro drift estimation errors (see equations 2.4-2.9). Between updates, this higher gyro drift error would degrade the attitude solution since the gyro data would compensated with an incorrect gyro drift estimate. The gyro scale factor errors and misalignments have no significant affect on the attitude solution since the spacecraft is inertially pointed and has no significant angular rates. As expected, the FHST misalignments have the largest affect on attitude accuracy. For both FHST #1 and #2, the misalignment of the X and Y tracker axes result in attitude estimation errors of over 70 arcseconds. Both FHSTs had a maximum attitude estimation error of 76 arcseconds when their Y-axis was misaligned. The increased FHST noise has only a small effect on the attitude error since there are sufficient measurements to reduce the scope of the error, and the system has good observability.

The attitude error results for the FHST/FSS cases are as follows:

Attitude Determination Errors (arcseconds)

Case	Axis	Roll	Pitch	Yaw

1B		127.21	121.30	74.65
2B	x	127.24	121.30	74.65
2B	y	127.24	121.40	74.65
2B	z	127.21	121.30	74.69
3B	x	128.04	120.13	80.12
3B	y	127.43	122.02	74.65
3B	z	127.21	121.30	74.91
4B	x	127.21	121.30	74.65
4B	y	127.21	121.30	74.65
4B	z	127.21	121.30	74.65
5B	x	127.21	121.30	74.65
5B	y	127.21	121.30	74.65
5B	z	127.21	121.30	74.65
6B	x	149.19	121.30	74.66
6B	y	127.21	121.30	91.91
6B	z	127.21	121.30	74.65
7B	x	208.19	209.49	74.76
7B	y	127.24	121.36	74.85
7B	z	127.21	121.33	74.65
8B		128.35	120.32	94.66
9B		131.64	126.30	74.93
10B		132.30	126.36	74.97

The gyro drift error results for the FHST/FSS case are as follows:

Gyro Drift Estimation Errors (10^{-3} arcseconds/second)

Case	Axis	Roll	Pitch	Yaw
1B		4.093	4.187	4.169
2B	x	4.147	4.183	4.169
2B	y	4.108	4.262	4.169
2B	z	4.093	4.187	4.248
3B	x	7.139	3.399	6.376
3B	y	4.277	6.653	4.169
3B	z	4.093	4.187	5.962
4B	x	4.093	4.187	4.169
4B	y	4.093	4.187	4.169
4B	z	4.093	4.187	4.169
5B	x	4.093	4.187	4.169
5B	y	4.093	4.187	4.169
5B	z	4.093	4.187	4.169
6B	x	4.093	4.187	4.169
6B	y	4.093	4.187	4.486
6B	z	4.093	4.187	4.169
7B	x	4.093	4.187	4.172
7B	y	4.093	4.187	6.534
7B	z	4.093	4.187	4.172
8B		5.195	3.838	5.767
9B		6.073	6.268	2.968
10B		6.343	6.329	3.533

As with the FHST/FHST simulations, an increase of gyro white noise or random walk about an axis primarily affects that axis. Not only does a correlation of the X and Y axes exist as in the FHST/FHST case, but a X and Z correlation exits. Of the two gyro noises, the random walk error has the largest affect on the attitude errors due

to attitude computations between measurement updates as mentioned in the previous case. The gyro scale factors and misalignments have no significant affect on the attitude or gyro bias errors due to the spacecraft being inertially pointed. The FHST #2 and FSS misalignments are the greatest contributors to attitude errors as expected since they define the attitude. The FSS affects the attitude errors more due to the greater alignment errors as compared to FHST # 2. Increasing the FHST noise results in the roll error increasing by 1 arcsecond, the pitch error decreasing by 1 arcsecond, and the yaw estimation error increasing by 20 arcseconds. The increased FHST noise to 64 arcseconds is much closer to the FSS measurement noise of 82 arcseconds. Thus, the FSS measurements would be weighted almost as much as the FHST measurements. The large FSS alignment uncertainties are then fed into the yaw estimation errors. The above maximum error occurs when the FHST is occulted which further degrades the yaw solution. Increasing the FSS noise increases the roll, pitch, and yaw estimation errors due to the limited memory of the filter to measurements. Thus, the measurement noise cannot be averaged out totally. The yaw error is only slightly higher than the baseline since any FSS is weighted much less than in the baseline while the FHST measurements are weighted the same. When the noise on the FSS and FHST are increased, the total error is due totally to the increased noise and the limited memory of the filter mentioned above.

The attitude error results for the 1 FHST with 2 Guide Stars are:

	Attitude Determination Errors (arcseconds)			
Case	Axis	Roll	Pitch	Yaw
1C		100.34	100.03	64.38
2C	x	100.43	100.07	64.38
2C	y	100.40	100.13	64.38
2C	z	100.34	100.03	64.56
3C	x	109.61	107.65	64.38
3C	y	108.02	109.23	64.38
3C	z	100.34	100.03	65.98
4C	x	100.34	100.03	64.38
4C	y	100.34	100.03	64.38
4C	z	100.34	100.03	64.38
5C	x	100.34	100.03	64.38
5C	y	100.34	100.03	64.38
5C	z	100.34	100.03	64.38
6C	x	107.77	107.46	64.38
6C	y	100.34	100.03	84.97
6C	z	107.77	107.43	64.38
7C		155.73	154.99	65.19

The gyro drift error results for the 1 FHST with 2 Guide Stars is:

	Gyro Drift Estimation Errors (10^{-3} arcseconds/second)			
Case	Axis	Roll	Pitch	Yaw
1C		5.378	5.375	3.382
2C	x	5.407	5.393	3.382

2C	y	5.396	5.400	3.382
2C	z	5.378	5.375	3.503
3C	x	8.856	6.653	3.382
3C	y	6.660	8.845	3.382
3C	z	5.378	5.375	6.394
4C	x	5.378	5.375	3.382
4C	y	5.378	5.375	3.382
4C	z	5.378	5.375	3.382
5C	x	5.378	5.375	3.382
5C	y	5.378	5.375	3.382
5C	z	5.378	5.375	3.382
6C	x	5.378	5.375	3.382
6C	y	5.378	5.375	3.382
6C	z	5.378	5.375	3.382
7C		6.811	6.804	3.694

As in the FHST/FHST case, an increases in the white and random walk noise about an axis primarly affects that axis. The correlation between the X and Y axes still exists. Of the two noises, the random walk has the largest affect on the attitude due to the increased gyro drift estimation error as mentioned above. The gyro scale factor error and misalignments as expected have no affect on the attitude estimation error. Also as expected, the added FHST alignment errors have a significant affect on the attitude estimation errors. The maximum attitude estimation error from the FHST misalignments is 107 arcseconds. The primary source of attitude estimation error is from the FHST noise. This results from the small separation of the guide stars in the FHST (2.8 degrees). The attitude estimation errors due to the measurement noise is an arctangent relationship seen in the following diagram (Reference 9):

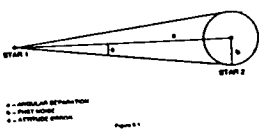

For this simulation, this error was approximately 1290 arcseconds. The RSS attitude estimation error for the noise simulation is approximately 229 arcseconds. The filter was able to improve the solution by 1061 arcseconds. The filter's memory for the measurements was not long enough to average out the measurement noise further.

Of the three cases simulated, the FHST/FHST case is by far the most accurate as expected. The choice for the backup case is not as easy to choice. The disadvange of the FHST/FSS case is the FSS alignment errors. Unless the FSS alignment is updated often, alignment errors due to thermal effects could degrade the attitude accuracy significantly. From an alignment point of view, the 1 FHST case is the most preferable due to the FHST being mounted on a fairly stable platform which is beside the gyros. From a noise point of view, the 1 FHST case is worse than the FHST/FSS case. The accuacy could be improved if more than two guide stars were available or the angular separation was larger. A possible solution to the problem is to use the 1 FHST case as a backup provided at least two guide stars are available and the FHST noise has not increased significantly from

launch. The alignment errors would be less than that for the FHST/FSS case and more of the sky would be open for viewing due to the limited FOV of the FSS. Otherwise, if the FHST noise has increased significantly since launch or there are not enough guide stars, use the FHST/FSS case.

6.0 OBC ATTITUDE ESTIMATION CALIBRATION AND VALIDATION

Nominal Operations

After the spacecraft has completed inorbit checkout, there are two phases for validating the onboard calculated attitude: post normal maneuver mode phase and normal pointing mode phase. Once the normal maneuver is performed, the onboard filter convergence needs to be validated. This convergence is defined as steady state operation and should occur within 3 hours of filter initialization (Reference 3). Once the filter has converged, the mission is in the normal pointing mode phase. According to Teledyne documentation, the acceleration insensitive drift rate (AIDR) peak over six hours is 0.0006 arcseconds/second (Reference 4). Assuming the update filter was disabled, the attitude errors due to the AIDR alone could be 51.84 arcseconds in 24 hours. This requires the onboard attitude estimation to be checked a minumum of once/day.

Before the procedure for validating the onboard attitude estimation process is discussed, the error comparison limits need to be determined. The GRO requirement for attitude determination is an absolute requirement. This absolute requirement references the attitude to the spacecraft body. An attitude sensor alignment can be determined relative to an optical cube on the ground. However once the spacecraft is placed on orbit, this alignment is unknown due to launch shocks. A ground system can align the attitude sensors relative to a reference attitude sensor. The attitude can be determined relative to the reference attitude sensor. The resulting attitude estimation error would be a function of the attitude sensors and attitude determination algorithm accuracies. This "relative" attitude estimation is what will be checked by the ground system since the alignment relative to body necessary for an "absolute" attitude estimate is unknown on the ground as well as onboard.

The portion of the TRW error budget devoted to algorithm errors is 53.3 arcseconds for FHST/FHST case and 66.3 arcseconds for the FHST/FSS case. The FHST and FSS noise allocations in the error budget are 10 and 24.1 arcseconds respectively. After RSSing the appropriate sensor noises with the associated algorithm errors for each case, the following comparison accuracy limits are obtained:

GRO ONBOARD ATTITUDE ESTIMATION ERROR COMPARISON LIMITS	
FHST/FHST	55.1 arcseconds/axis
FHST/FSS	71.2 arcseconds/axis

Figure 6.1

The onboard attitude estimate will be compared to the attitude

estimate from the Code 550 Fine Attitude Determination System (FADS). An outline for the comparison procedure is as follows:

1) Select an orbit of data.
2) Process the sensor data through a batch least squares filter to obtain a ground attitude estimate.
3) Compute errors between the ground attitude estimate and the OBC estimate.
4) Compare these errors to the comparison numbers in Figure 6.1.
5) If the attitude errors are less than those in Figure 6.1, then the OBC attitude estimation function is operating properly, and the validation process is complete.
6) If the attitude errors are greater than those in Figure 6.1, follow steps 7-9 since the the OBC may not be functioning properly.
7) Check to see if the attitude estimate is diverging from the ground solution. If not, then the filter needs tuning.
8) Check to see if any of the following attitude sensors have failed or if the sensor data is degraded:
    a) Gyros
    b) FHSTs
    c) FSS
9) Check to see if the FHST(s) are tracking stars for less than 32.768 seconds. If this is happening, then there could be a star match problem. This could mean a bad onboard covariance (filter tuning probably required), failure of the FHST, or a bad uplink of guide stars. The update filter validates an observed star only if matches with <u>one</u> uplinked guide star. A lack of a guide star match or a match with more than guide star causes the update filter to send a break track command to search for a new star.

At the time these tests are being performed, all update filter data base parameters need to be checked for the previous 24 hour period. Bad data base updates could easily upset onboard attitude estimation.

<u>Contingencies</u>

If the attitude estimation errors equal or exceed comparison limits and the possible problems discussed above have been eliminated, OBC attitude determination calibration may be required. The Onboard filter can be calibrated by the following methods:

a) tuning parameter adjustment
b) changing update frequency of covariance matrix
c) changing measurement frequency

Onboard filter calibration can most easily be performed by tuning parameter adjustment. Short of modifying the Onboard filter, the tuning parameters are the following:

a) Initial Attitude errors along the covariance diagonal
b) Initial Gyro Drift errors along the covariance diagonal
c) FHST noise variance
d) FSS noise variance
e) Gyro white noise estimate.
f) Gyro random walk estimate.

The initial attitude and gyro drift errors in the state covariance matrix occupy the first six diagonal elements. These are data base constants that are used to initialize the state covariance matrix when the filter is initialized. The more accurate these numbers are, the faster the filter will converge to the correct solution. Since the largest value of the upper lefthand 3x3 matrix are used for star selection criteria, a good estimate of the initial attitude and gyro drift errors will decrease the possibility of a misidentification of a star.

The sensor noise variances are used in determining the weight of a particular measurement. This can be seen in the GRO Kalman gain equation:

$$K_{k,i} = P_{k,i}(-)\ H_{k,i}^T \ /\ [\ H_{k,i}\ P_{k,i}(-)\ H_{k,i}^T + R_{k,i}\ ] \qquad (6.1)$$

where $R_{k,i}$ is the sensor noise for a particular measurement. If $R_{k,i}$ is increased, then the Kalman gain K_k will be decreased and more emphasis will be placed on the estimate $X_k(-)$:

$$\hat{\underline{X}}_k(+) = \hat{\underline{X}}_k(-) + K_k\ (\ \underline{Z}_k - H_k\ \hat{\underline{X}}_k(-)\ ) \qquad (6.2)$$

This allows the filter to place emphasis on more accurate measurements. In the FHST/FSS case, the FHST measurements would be given more confidence by the filter than the FSS measurements since FHSTs are more accurate. The estimated dynamic noise for the filter (white noise and random walk) come into play with the propagation of the state covariance matrix. The spectral density matrix is defined as follows:

$$Q(t) = E\ [\ \underline{W}(t)\ \underline{W}^T(t)\ ] \qquad (6.3)$$

where $\underline{W}(t)$ is white noise vector in the state equation (2.3). $Q(t)$ is used to form the discrete dynamics noise covariance matrix as follows:

$$Q_k = \int_{t_{k-1}}^{t_k} \phi(t_k,t')\ Q(t')\ \phi^T(t_k,t')\ dt' \qquad (6.4)$$

which is used in the propagation of the covariance matrix as follows

$$P_k(-) = \phi_k\ P_{k-1}(+)\ \phi_k^T + Q_k \qquad (6.5)$$

Calibration Method	Table Parameters	FDF Control?	Comments
TUNING PARAMETERS			
FHST Noise Var.	Table 37	YES	Useful if FHST data is noisy or to add weight to the FSS measurements
FSS Noise Var.	Table 42	NO	Useful if FSS data is noisy or to add weight to the FHST measurements
Initial attitude errors	Table 42	NO	Useful for the convergence of the filter
Initial gyro drift errors	Table 42	NO	Useful for the convergence of the filter
White noise	Table 36	YES	Needed if gyro white noise increases or if less emphasis on the dynamic model is desired
Random walk	Table 36	YES	Needed if gyro random walk noise increases or if less emphasis on the dynamic model is desired
Related Parameters			
Estimated attitude errors	Table 42	NO	Useful for small onboard attitude quaternion corrections.
Estimated gyro drift errors	Table 42	NO	Needed to insure the onboard attitude is propagated correctly.
Attitude quaternion	Table 59	NO	Needed if onboard quaternion is bad
OTHER METHODS			
Covariance Update Frequency Change	N/A	N/A	Requires code changes in ATTEST and probably the EXEC routine. Not an easy modification.
Measurement Update Frequency Change	N/A	N/A	Requires changes in the EXEC routine. Probable OBC loading problems.

Table 6.1 Update Filter Calibration Method Summary

The progagation of the covariance matrix is used in the computation of the Kalman gain as can be seen in equation (6.1) as well as the star identification process mentioned above. Since the Kalman gain is used to determine the updated state vector (6.2), $P_k(-)$ has potential to undermine the state estimation process if poorly computed.

The second possible calibration method is changing the update frequency of the state covariance matrix (6.5). Currently, the onboard filter updates $P_k(-)$ every 32.768 seconds before the star identification process occurs. Increasing the update frequency could assist in state estimation as well as star identification. The state covariance matrix update is embedded in ATTEST which makes this possibility difficult to implement due to the software mods needed.

The last calibration method mentioned deals with measurement updates. Stellar updates very accurately pin down attitude errors and gyro drift errors. Gyro drift errors affect the attitude between measurement updates. During periods of no measurement updates, the onboard quaternion would be updated in the kinematic integration routine which uses slowly degrading gyro data. The gyro data used requires an accuate estimate of the gyro drift error to compensate the incremental angles. Without accurate gyro drift compensation, the onboard attitude quaternion would slowly diverge from the proper attitude. Now if measurement updates were made more frequently, the attitude would be compensated before it could degrade significantly. This modification would be easier to perform than changing the propagation frequency of the state covariance matrix since little coding changes would be required. The resulting OBC loading would need to be studied to determine whether this modification is viable.

7.0 CONCLUSIONS

For both the FHST/FHST and FHST/FSS configurations, the GRO onboard attitude determination accuracies can be met with significant margins (assuming nominal on-orbit conditions). For the FHST/FHST configuration, the roll, pitch, and yaw predicted attitude estimation errors are 64.11, 64.74, and 60.80 arcseconds respectively. The requirement is 86 arcseconds/axis. For the FHST/FSS configuration, the roll, pitch, and yaw predicted attitude estimation errors are 127.21, 121.30, and 74.65 arcseconds respectively. The requirement is 167.5 arcseconds/axis. For the 1 FHST with 2 guide star case, the attitude estimation errors were 100.34, 100.03, and 64.38 arcseconds respectively.

As expected for the FHST/FHST and FHST/FSS cases, the attitude estimation accuracies are most sensitive to FHST and FSS alignment errors. The gyro drift errors are most sensitive to random walk errors in both cases, but alignment errors provide the second largest component of gyro drift error. These results emphasize the importance of proper attitude sensor alignment determination.

The single FHST case demonstrated that onboard attitude estimation

rivalling that of the FHST/FSS combination is possible. However, this choice is highly sensitive to measurement noise. If the measurement noise is nominal and two guide stars are available, it is recommended to use this case over the FHST/FSS case due to high FSS alignment errors and the FSS FOV limitation on target attitudes.

A procedure was outlined for GRO OBC attitude estimation validation. It was pointed out that the accuracy check is a relative check and not an absolute check. The attitude error comparison for the FHST/FHST case is 55.1 arcseconds/axis and 71.2 arcseconds/axis for the FHST/FSS case.

When and if problems with the onboard attitude estimation process are detected, three onboard filter calibration techniques are available: filter tuning, increased state covariance matrix update frequency, and increased ATTEST frequency. Of the three techniques, filter tuning parameter adjustment is the easiest. In extreme situations where filter turning is not sufficient, an increased measurement frequency for ATTEST would require the least software modifications. OBC loading would need to be studied though since ATTEST is the largest function in the Attitude Control and Determination (ACAD) portion of the OBC flight software.

10.0 REFERENCES

1. Snow, Harman, Garrick, "An Analysis of the Kalman Filter in the Gamma Ray Observatory (GRO) Onboard Attitude Determination Subsystem," NASA/GODDARD SPACE FLIGHT CENTER FLIGHT MECHANICS/ ESTIMATION SYMPOSIUM 1988, May 10-11.
2. Wertz, James, edit., SPACECRAFT ATTITUDE DETERMINATION AND CONTROL, D. Reidel Publishing Company, 1985.
3. TRW, 40420-86-322-001, GRO OPERATIONS DATA BOOK PART 3 - ACAD SUBSYSTEM VOLUME II, 2 Sept. 1986.
4. Kulp, D., "IRU calibration Analysis", SEAS QUICK NOTE NO.: EUVE-413-90003, October 27, 1989.
5. Teledyne Systems Company, "NASA Standard High Performance Inertial Reference Unit DRIRU II", January 1988.
6. Jayaraman, C. and Braunstein, K., "Explorer Platform Star Tracker Calibration", Fairchild Interoffice Communication, ACS:EP:89:080, July 19, 1989.
7. Torgow, Joan S., USERS' GUIDE TO THE STANDARD STAR Configuration, Performance, and Use, TM86-02, Ball Aerospace Division, April 1986.
8. TRW, EQ7-145, EQUIPMENT SPECIFICATION FINE SUN SENSOR ASSEMBLY, 22 August 1983.
9. Convesation with F. Landis Markley, NASA/GSFC Code 712.1, December 13, 1989.
10. Harman, R, GRO MISSION FLIGHT DYNAMICS ANALYSIS REPORT: Onboard Computer (OBC) Attitude Error Analysis (Analysis Item No. A1.2), Mission Report 90004N.